

Li-rich RGB stars in the Galactic Bulge

O. A. Gonzalez^{1,2}, M. Zoccali¹, L. Monaco³, V. Hill⁴, S. Cassisi⁵, D. Minniti^{1,6}, A. Renzini⁷, B. Barbuy⁸, S. Ortolani⁹,
and A. Gomez¹⁰

¹Departamento Astronomía y Astrofísica, Pontificia Universidad Católica de Chile, Av. Vicuña Mackenna 4860, Stgo., Chile
e-mail: oagonzal@uc.cl; mzoccali@astro.puc.cl; Dante@astro.puc.cl

²European Southern Observatory, Karl-Schwarzschild-Strasse 2, D-85748 Garching, Germany

³Departamento Ciencias Físicas y Astronómicas, Universidad de Concepción, Concepción, Chile
e-mail: lmonaco@astro-udec.cl

⁴Université de Nice Sophia Antipolis, CNRS, Observatoire de la Côte d'Azur, B.P. 4229, 06304 Nice Cedex 4, France
e-mail: vanessa.hill@obspm.fr

⁵INAF-Osservatorio Astronomico di Teramo, via M. Maggini, 64100 Teramo, Italy
e-mail: cassisi@oa-teramo.inaf.it

⁶Specola Vaticana, V00120 Citta del Vaticano, Italy

⁷INAF-Osservatorio Astronomico di Padova, Vicolo dell'Osservatorio 2,I-35122 Padova, Italy
e-mail: alvio.renzini@oapd.inaf.it

⁸Universidade de São Paulo, IAG, Rua do Matão 1226, Cidade Universitária, São Paulo 05508-900, Brazil
e-mail: Barbuy@astro.iag.usp.br

⁹Università di Padova, Dipartimento di Astronomia, Vicolo dell'Osservatorio 5,I-35122 Padova, Italy
e-mail: sergio.ortolani@unipd.it

¹⁰Observatoire de Paris-Meudon, 92195 Meudon Cedex, France
e-mail: Ana.Gomez@obspm.fr

Received 05 May 2009; Accepted 09 July 2009

ABSTRACT

Aims. We present Lithium abundance determination for a sample of K giant stars in the galactic bulge. The stars presented here are the only 13 stars with detectable Lithium line (6767.18Å) among ~400 stars for which we have spectra in this wavelength range, half of them in Baade's Window ($b = -4^\circ$) and half in a field at $b = -6^\circ$.

Methods. The stars were observed with the GIRAFFE spectrograph of FLAMES@VLT, with a spectral resolution of $R \sim 20,000$. Abundances were derived via spectral synthesis and the results are compared with those for stars with similar parameters, but no detectable Li line.

Results. We find 13 stars with a detectable Li line, among which 2 have abundances $A(\text{Li}) > 2.7$. No clear correlations were found between the Li abundance and those of other elements. With the exception of the two most Li rich stars, the others follow a fairly tight $A(\text{Li}) - T_{\text{eff}}$ correlation.

Conclusions. It would seem that there must be a Li production phase during the red giant branch (RGB), acting either on a very short timescale, or selectively only in some stars. The proposed Li production phase associated with the RGB bump cannot be excluded, although our targets are significantly brighter than the predicted RGB bump magnitude for a population at 8 kpc.

Key words. Stars: abundances, late-type - Galaxy: bulge

1. Introduction

The cosmic evolution of Lithium has been a matter of debate in the recent past, due to some marked inconsistencies between its predicted abundance and a few key observations (see, e.g., Cyburt et al. 2008 for a recent review).

The dominant lithium isotope is ${}^7\text{Li}$, which is thought to be produced by Big Bang nucleosynthesis, up to abundance $A(\text{Li}) \sim 2.2$, i.e., the so-called Spite plateau abundance observed in the surface of metal-poor stars. Since then, Li has been produced by hot bottom burning (Sackmann & Boothroyd, 1999) during the asymptotic giant branch (AGB) evolution of intermediate mass stars ($> 4M_{\odot}$), or by cosmic ray spallation, but also destroyed in stellar interiors where temperatures are in excess of $2.0 \times 10^6\text{K}$.

In this context, a typical bulge star of roughly solar metallicity is expected to begin its life, on the main sequence, with a Li abundance close to $A(\text{Li}) = 3.0$. During the first dredge up, when envelope convection penetrates down to high temperature regions, Li is partly destroyed (diluted) by ~ 1.5 dex (Iben 1967a,b) so that typical near solar metallicity RGB stars are expected to have $A(\text{Li}) < 1.5$. However, stars on the upper RGB are expected to be more Li depleted due to the extra-mixing observed to start acting at the RGB bump (Gratton et al. 2000, Lind et al. 2009b). In marked contrast with this expectation, several Li rich red giants have been found to date, both in clusters and in the field (e.g., McKellar 1940; Faraggiana 1991; Smith et al. 1995; Hill & Pasquini 1999; Kraft & Shetrone 2000; Domínguez et al. 2004; Monaco & Bonifacio 2008).

As a possible explanation for this evidence, a Li production phase during the RGB via Cameron-Fowler mecha-

nism (Cameron & Fowler 1971) has been proposed (Sackmann & Boothroyd 1999, Charbonnel & Balachandran 2000, Denissenkov & Herwig 2004). In order to synthesize Li in stellar interiors, two conditions are required. First, temperature should be hot enough for the reaction ${}^3\text{He}(\alpha, \gamma){}^7\text{Be}$ to occur. Second, ${}^7\text{Be}$ must be quickly transported to cooler regions where Li can be produced by the ${}^7\text{Be}(e^-, \nu){}^7\text{Li}$ reaction. Thus, the reaction producing Be should occur very close to some convective region, or, alternatively, convection should penetrate into some burning shell. Then, in low mass stars, some kind of extra-mixing must circulate the material from the convective envelope to a region close to the H-burning shell. The source of this extra-mixing has been related to shear instabilities, meridional circulation or diffusion.

Charbonnel & Balachandran (2000) show that a significant number of Li rich giants appear to be located close to the RGB bump where an extra-mixing process is observed to strongly affect the abundances of C, ${}^{12}\text{C}/{}^{13}\text{C}$ and N (Gratton et al. 2000, Gratton, Sneden & Carretta 2004). Based on this evidence, they propose a scenario where, while the H-burning shell erases the molecular weight discontinuity left by the penetration of the convective envelope during the first dredge up, the extra-mixing could circulate the material in order to produce Li. Once mixing proceeds long enough to produce the observed dip in the carbon isotopic ratio during and after the RGB bump, the fresh ${}^7\text{Li}$ would be quickly destroyed, such that the Li rich phase would be a very short one. This latter point would explain why only a small fraction of the observed RGB stars are actually Li rich. However, so far this qualitative explanation could not be reproduced by models accounting for rotational distortions (Palacios et al. 2006) and it is also challenged by some observation of Li rich stars significantly brighter than the RGB bump (Monaco & Bonifacio 2008, Kraft et al. 1999)

Sackmann & Boothroyd (1999) suggested that, under certain conditions, an increase in the Li abundance could be produced by a deep circulation mechanism after the molecular weight barrier is erased. Therefore, depending on the extra-mixing details, Li-rich red giants may be found at any location of the RGB. However, the problem arises when comparing the behavior of other elements, in particular ${}^{12}\text{C}/{}^{13}\text{C}$, with the expected values from their proposed model. In particular, in their scenario the lower ${}^{12}\text{C}/{}^{13}\text{C}$ value is only reached at the tip of the RGB and not right after the RGB bump as observed (Gratton, Sneden & Carretta 2004).

Alternatively, Denissenkov & Herwig (2004) proposed a distinction between the extra-mixing at the RGB bump and a so called enhanced extra-mixing induced by rotation that could be triggered by the spinning up by an external source of angular momentum which then could increase the Li abundance.

Other explanations for Li rich red giants have been proposed, such as some mechanism that might prevent Li dilution during the first dredge up, or contamination by possible planets. However, both phenomena would imply enrichment of ${}^9\text{Be}$ (in addition to ${}^6\text{Li}$ and ${}^{11}\text{B}$) which is not usually observed in Li rich stars (Melo et al. 2006). Therefore, the internal Li production during the RGB via Cameron-Fowler mechanism seems to be the most likely scenario to explain low mass Li-rich giants.

Recently, two different sources of extra mixing have been proposed in order to reproduce the observed changes in surface abundances. Thermohaline mixing triggered by a double diffusive instability (Charbonnel & Zahn 2007a) and magneto-thermohaline mixing (Denissenkov et al. 2009) induced by magnetic buoyancy. While the way in which thermohaline mixing may account for observed Li rich giants has not been yet ex-

Table 1. Bulge fields characteristics

N	Name	l	b	R_{GC}	E(B-V)
1	Baade's Window	1.14	-4.18	604	0.55
2	$b = -6^\circ$	0.21	-6.02	850	0.48

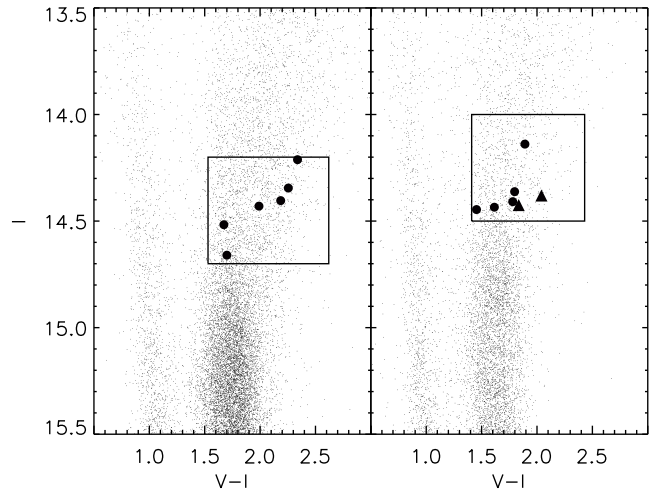


Fig. 1. Color magnitude diagram for both fields, baade's window (left) and $b=-6$ (right) with the positions of the Li rich stars from our sample marked as large filled circles. The two stars showing the higher Li abundances are marked as large filled triangles. Magnitudes were obtained from OGLE catalogue (Udalski et al. 2002) and Zoccali et al. 2008 catalogue obtained from WFI images

plained, Guandalini et al. (2009) has shown that mixing induced by magnetic buoyancy might explain the observation of both Li-rich and Li-poor stars along the RGB. However, a deeper understanding of magnetic fields in low mass giants as well as a larger sample of Li rich RGB stars are required to confirm these results.

Here we present Li abundances for 13 stars with detectable Li, observed in the context of our survey of RGB stars in the Galactic bulge (see Zoccali et al. 2008 and Lecureur et al. 2007 for a description of the whole project).

2. RGB Sample

The spectra discussed here have been obtained in the context of a larger FLAMES-GIRAFFE survey of bulge K giants, in four fields (c.f. Zoccali et al. 2008). Only two of the fields, namely Baade's Window and the field at $b = -6^\circ$ have been observed with the HR15 setup, including the Li line at 6707.18 \AA . The S/N ranges from 40 to 90 and the resolution is $R \sim 20,000$. In total, we have measured Li in $204 + 213 = 417$ bulge giants, whose location in the color magnitude diagram (CMD) is shown in Fig. 1. Only 13 of those stars showed a detectable Li line, thus the following analysis will concentrate on them, that we will call "Li rich" stars¹.

¹ Note that the name "Li rich" has been often used for giants having $A(\text{Li}) > 1.5$. Only 6 of our stars show such high abundances, but we extend here the name to all the stars having detectable Li, in contrast with the other ~ 400 giants for which we could see no line at all.

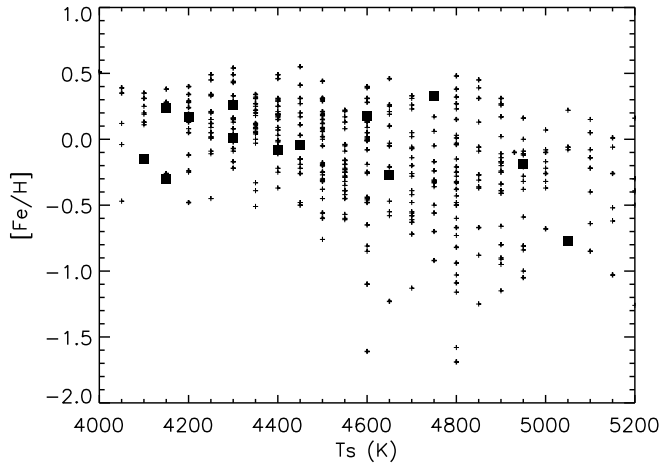


Fig. 2. Metallicity versus effective temperature diagram for all the observed bulge giants (small crosses) in both fields. Li rich giants are shown as big filled squares)

Stellar parameters were obtained from Zoccali et al. (2008). As can be seen from Fig. 2, observed stars have effective temperature varying from 4000 to 5200 K and iron content, $[Fe/H]$, between -1.7 and $+0.5$. Li rich stars span the whole temperature range, while their rather high metallicity is consistent with the small sampling of a metallicity distribution peaked close to solar metallicity.

3. Spectral synthesis and Li abundances

For the 13 stars showing a detectable line, Li abundances were determined by comparison with synthetic spectra created with MOOG (Snedden, 2002). MOOG is a FORTRAN code that performs spectral line analysis and spectrum synthesis task under local thermal equilibrium approximation. MARCS model atmospheres (Gustafsson 2008) were created using the stellar parameters given in Table 2.

3.1. Linelists

The TiO molecular linelist (Plez, 1998) used by Lecureur et al. (2007) was included, but those lines turned out to be negligible in the relevant wavelength range. CN lines are stronger, especially for cold stars. The Kurucz CN linelist was obtained from the Kurucz database. Atomic lines in the vicinity of the Li line were obtained from Reddy et al. 2002.

Once all linelists were compiled, the $\log gf$ values of the CN and atomic lines within 8 \AA from the Li line were modified to reproduce the observed spectra of Arcturus and μ Leonis, as shown in Fig. 3 using the abundances given in Lecureur et al (2007). The $\log gf$ value for Ti I line at 6708.025 \AA was modified from the adopted by Reddy et al. 2002 as well as both V I lines at 6708.125 \AA and 6708.280 \AA . The final, calibrated atomic lines used for the synthesis are listed in Table 2.

3.2. Synthesis

Synthetic spectra were computed for each Li rich star using the corresponding stellar parameters and iron content listed in Table

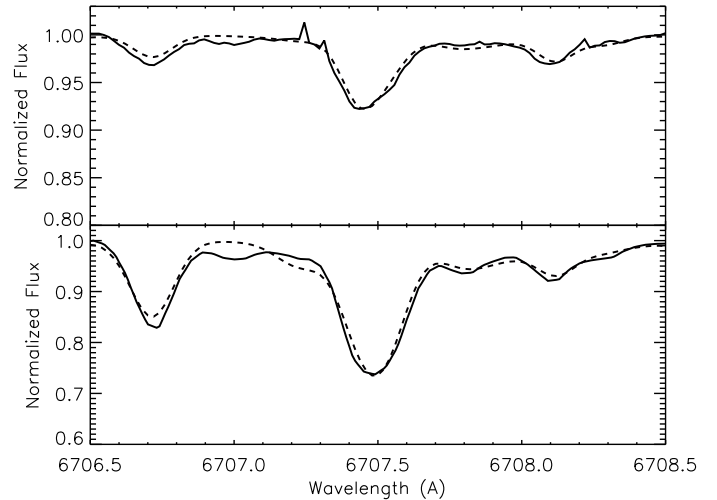


Fig. 3. Observed spectra as solid line and synthetic spectra as dashed line for Arcturus (upper panel) and for μ Leonis (lower panel) used for calibration of the $\log gf$ values for lines in the vicinity of the Li line

Table 2. Atomic linelist in the vicinity of the lithium line, used for this study

λ (\AA)	Element	χ_{ex}	$\log gf$
6707.4331	Fe I	4.610	-2.300
6707.4500	Sm II	0.930	-3.140
6707.5630	V I	2.740	-1.530
6707.6440	Cr I	4.210	-2.140
6707.7400	Ce II	0.500	-3.810
6707.7520	Ti I	4.050	-2.654
6707.7561	^7Li	0.000	-0.428
6707.7682	^7Li	0.000	-0.206
6707.7710	Ca I	5.800	-4.015
6707.9066	^7Li	0.000	-1.509
6707.9080	^7Li	0.000	-0.807
6707.9187	^7Li	0.000	-0.807
6707.9200	^7Li	0.000	-0.807
6708.0250	Ti I	1.880	-4.252
6708.1001	V I	1.220	-3.200
6708.1250	Ti I	1.880	-2.886
6708.2800	V I	1.220	-3.178

4. The abundances of C,N and O were obtained from Lecureur et al. (2007), where, based on a subsample of stars observed at higher resolution with UVES, approximate relations were derived between the abundances of CNO and $[Fe/H]$. All other abundance ratios were scaled to the stellar metallicity assuming a solar mix (Grevesse & Sauval, 1998). The observed spectra were corrected by the radial velocities obtained from DAOSPEC (Stetson & Pancino 2008) and checked for telluric lines in the Li range. Each synthetic spectrum was compared to the observed one in two steps. First, a 10 \AA window was used to perform a correct normalization to the continuum around the Li line. Second, a smaller window (4 \AA) was used to reproduce the Li line, iteratively modifying only the Li abundance until the best fitting value was reached. Additionally, NLTE corrections were calcu-

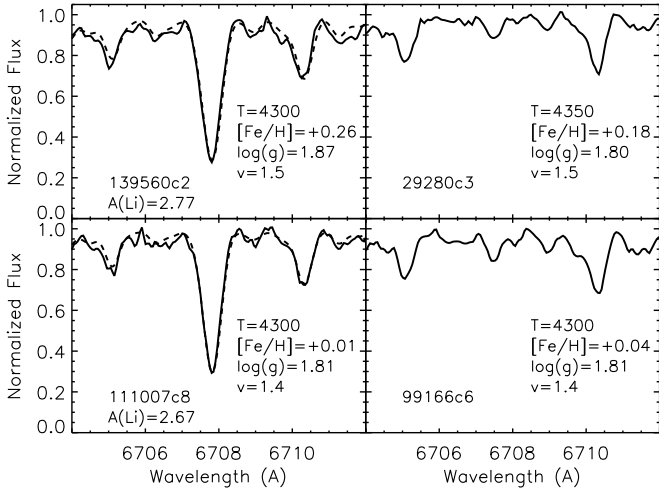


Fig. 4. *Left panels:* Observed (solid line) and synthetic (dashed line) spectra for the two most Li-rich stars found from the sample. *Right panels:* Observed spectra for two stars with similar T_{eff} , $[\text{Fe}/\text{H}]$, v_t and $\log g$ to both Li rich stars, but no ${}^7\text{Li}$ line present.

Table 4. Stellar parameters and determined Li abundance to the sub-sample of stars with a distinguishable Li line

N	ID	$\log g$	v_t	T_s	$[\text{Fe}/\text{H}]$	$A(\text{Li})_{\text{LTE}}$	$A(\text{Li})_{\text{NLTE}}$
1	82831	1.99	1.4	4750	0.33	1.74	1.98
2	205356	2.16	1.5	4950	-0.19	1.87	2.04
3	564760	1.74	1.3	4150	-0.30	0.77	1.08
4	564789	1.70	1.2	4100	-0.15	0.66	1.00
5	231128	1.76	1.4	4200	0.17	0.80	1.14
6	392931	1.89	1.5	4450	-0.04	1.13	1.45
7	108191c7	2.11	1.5	5050	-0.77	2.17	2.24
8	69986c2	2.01	1.5	4650	-0.27	1.21	1.46
9	139560c2	1.87	1.5	4300	0.26	2.77	2.78
10	103413c6	1.65	1.4	4150	0.24	1.01	1.34
11	75601c7	1.79	1.5	4400	-0.08	0.78	1.11
12	77419c7	1.93	1.5	4600	0.18	1.54	1.82
13	111007c8	1.81	1.4	4300	0.01	2.67	2.68

lated by interpolation the in grids by Lind et al. (2009), for the stellar parameters of each one of the Li rich stars².

The derived LTE and NLTE Li abundances for the 13 Li rich stars are listed in the last two columns of Table 4. The two stars showing extremely high Li abundances, $A(\text{Li}) \sim 2.7$, are showed in the left panels of Fig. 4 along with the best fitting synthetic spectrum. Additionally we performed spectral synthesis to other six stars from each field, spanning the whole parameter range of the Li rich sample, in order to obtain reference upper limit Li abundance for *normal* stars.

The errors on the measured Li abundances were obtained by varying each of the stellar parameters by its estimated error, and re-determining the Li abundance. The largest uncertainty is associated to the effective temperature, whose error is estimated to be $\pm 200\text{K}$ (Zoccali et al. 2008), implying a $\Delta A(\text{Li}) \sim 0.25$ dex for the hottest of our stars (see Table 3).

² NLTE corrections in Lind et al. 2009 are only available up to solar metallicity. Therefore, corrections for supersolar metallicity stars were calculated assuming $[\text{Fe}/\text{H}] = 0$

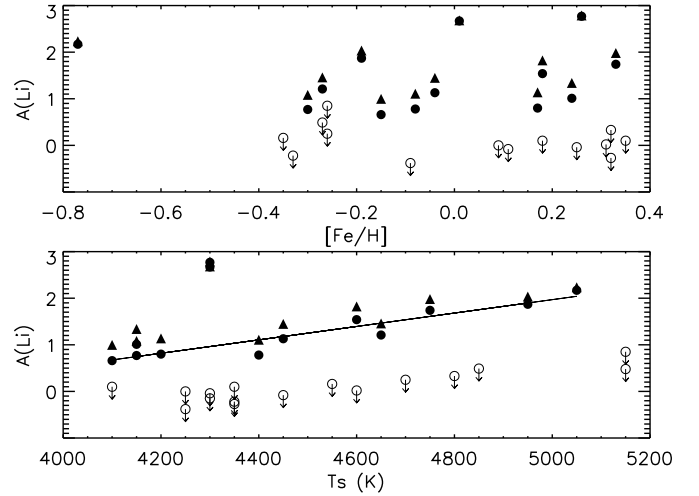


Fig. 5. Li_{LTE} (filled circles) and Li_{NLTE} (filled triangles) abundances and stellar parameters for the Li rich stars. Upper limits in $A(\text{Li})$ for a sample of random stars are shown as empty circles. No correlation is seen between lithium abundances and metallicity (upper panel). A clear correlation is visible between $A(\text{Li})$ and T_{eff} (lower panel) with the only two outliers being the most Li rich stars. A linear fit to the data gives a slope of 0.14 ± 0.02 dex/100 K.

4. Possible origin of a high Li abundance

4.1. Correlations with temperature and metallicity

In an attempt to understand the reason for the high Li observed in 13 of our stars, we investigate possible correlations between the derived Li content and the stellar parameters.

From the location of the Li rich stars in the CMD (Fig. 1) we see that they span the full color range of the other sample stars, and they do not clump in magnitude either. This information, coupled with their uniform spatial distribution -and similar number in both fields- allows us to exclude that they might belong to a different, peculiar, stellar population such as a star cluster.

All our Li rich stars have metallicities in excess of $[\text{Fe}/\text{H}] \sim -0.3$ with the exception of one star at $[\text{Fe}/\text{H}] = -0.77$ (Fig. 5). Given the global iron distribution function in these two fields (Zoccali et al. 2008) this is entirely consistent with (small) random sampling.

The temperature distribution of Li rich stars is extremely uniform across the whole range sampled by our targets, from 4000 to 5200 K. Very interestingly, with the exception of the two extremely Li rich stars shown in Fig. 4, all the other stars show a rather tight correlation between $A(\text{Li})$ and T_{eff} , as already found by Brown et al. (1989) in a survey of 644 giants in the DDO photometric catalog, Pilachowski et al. (1986) in NGC 7789 and Pilachowski et al. (1988) in M67 giants.

In order to ensure that the observed relation is real and is not produced by the reduced sensitivity to Li detections at hotter temperatures (thereby introducing correlated errors in T_{eff} and $A(\text{Li})$), we analyse here the effect that an error in temperature might introduce on the derived abundances.

Table 3 lists the variation of $A(\text{Li})$ due to an error of 200 K in the temperature of the adopted model atmosphere. It appears that an increase in temperature would imply an increase in the derived $A(\text{Li})$, and vice versa, thus artificially introducing a pos-

Table 3. Li Abundance errors associated to the uncertainties in stellar parameters

T (K)	ΔT		$\Delta \log g$		Δv_r		$\Delta [\text{Fe}/\text{H}]$	
	-200K	+200K	-0.3dex	+0.3dex	-0.2km/s	+0.2km/s	-0.2dex	+0.2dex
4200	-0.15	0.20	-0.01	0.02	0.00	0.00	0.15	-0.14
4650	-0.20	0.20	-0.01	0.01	0.00	0.00	0.20	-0.16
4950	-0.25	0.25	-0.01	0.01	0.00	0.00	0.23	-0.25

itive slope in the lower panel of Fig. 5. According to Magain (1984), the slope due to correlated errors would be given by:

$$\langle \delta f \rangle = c \frac{\sigma_c^2}{\sigma_T^2}$$

where:

$c = \frac{\partial A(\text{Li})}{\partial T} = 0.25 \text{ dex}/200\text{K}$ describes how $A(\text{Li})$ is correlated with T_{eff} , assuming the maximum variation, obtained for $T > 4950$;

$\sigma_T = 200 \text{ K}$ is the typical error in effective temperature;

and $\sigma_T = 333 \text{ K}$ is the variance of the effective temperature range

This gives an expected error in the slope due to correlated errors of $\langle \delta f \rangle \sim 0.1 \text{ dex}/200\text{K}$. The best fit for the data gives as slope of 0.28 dex in 200 K. Therefore most of the observed trend is certainly real.

Considering the hypothesis proposed Charbonnel & Balachandran (2000), the RGB bump should act as the evolutive instance in which we can separate the stars in three groups according to their Li content. i) Stars under standard dilution should be less evolved than the RGB bump and therefore could show the observed trend in Fig. 5; ii) stars under fresh Li production which should be located at the first instances of the RGB bump before full mixing takes place; and iii) stars which have left the RGB bump and no Li content should be observed on their surfaces. Thus, Li rich stars should be located, in the CMD, very close to the RGB bump. However, our stars, being in principle highly more evolved than RGB bump stars, obviously do not fit this scenario. In this context, the observed decline in lithium with temperature observed in our stars, can only be interpreted as the result of a process occurring as they evolve through the giant branch.

4.2. The evolutionary status of the Li-rich stars

Two of the stars have $A(\text{Li}) \sim 2.7$ and they fall always above the observed trend. Similar abundances of Li have been previously found in two giants by Brown et al. (1989). According to Charbonnel & Balachandran (2000) the latter two stars belong to the RGB bump. Since they also showed Be and ^6Li depletion, they were interpreted as having recently undergone a Li production phase. The fact that they had normal $^{12}\text{C}/^{13}\text{C}$ ratios, then, was thought to support the idea that Li production should precede the extra-mixing process lowering the carbon isotopic ratio. Our stars are brighter than the expected location of the RGB bump, if they are at the bulge mean distance. Therefore, the only way for them to fit in this scenario would be that they are in fact much closer, at $\sim 5 \text{ kpc}$ instead of 8 (see below).

Our target selection box in the CMD is located about 0.7 magnitudes above the horizontal branch red clump, at $V_{\text{box}} \sim 16.1$. For a solar metallicity population, the expected $\Delta V_{\text{HB}}^{\text{bump}}$ is 0.5 magnitudes (Zoccali et al. 1999). Since the observed red

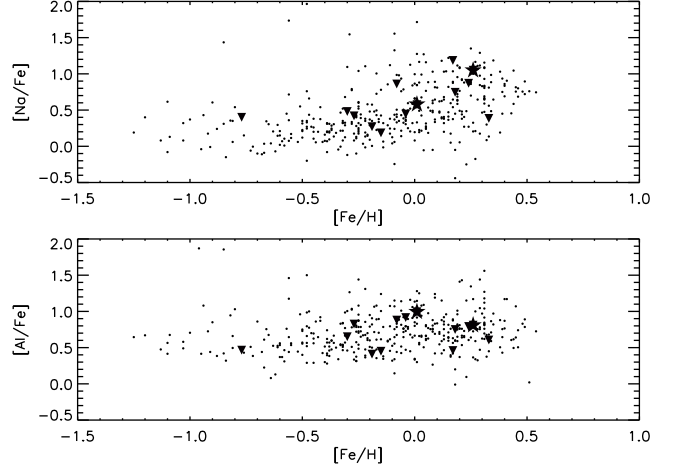


Fig. 6. $[\text{Na}/\text{Fe}]$ and $[\text{Al}/\text{Fe}]$ ratios versus metallicity. The full sample is plotted as small circles, the Li rich stars as filled triangles and the two most Li rich stars as filled stars.

clump is at $V \sim 16.8$, the RGB bump should then be at $V \sim 17.3$, i.e., 1.2 mag fainter than our target box. Even considering that the RGB bump occurs at brighter luminosities for metal poor stars, not even for the most metal poor Li rich star in our sample, the observed magnitude is compatible with the expected location of the RGB bump. Assuming a mean bulge distance of 8 kpc, Li rich stars in our sample should be at $\sim 4.6 \text{ kpc}$ from us in order to actually belong to the RGB bump. The bulge density at 3.4 kpc from the galactic center is very low (Rattenbury et al. 2007). Therefore, although this possibility cannot be excluded, it is rather unlikely.

More likely, these stars might be *disk* RGB bump stars, at $\sim 4.6 \text{ kpc}$ from us. In principle one way to separate bulge from disk stars might be their alpha element abundances. It has been found that $[\alpha/\text{Fe}]$ ratios appear to be higher for bulge stars than those belonging to the disk (e.g. Zoccali et al. 2006, Lecureur et al. 2007). If oxygen cannot be measured at the resolution of GIRAFFE, we can measure Mg, Al, and Na and check if they are lower than expected for bulge stars. Figure 6 shows that this is not the case, at least for Al and Na.

4.3. Binary nature

Costa et al. (2002) found that the Li abundances in binary systems including a giant show a trend with temperature similar to the one shown in Fig. 5. This fact was interpreted as tidal interactions influencing standard dilution. In fact, binary systems with synchronized rotational and orbital motions show higher lithium compared to non-synchronized binaries. In order to check for binarity in our targets, we looked for radial velocity variations among the individual spectra, before co-addition. For each ob-

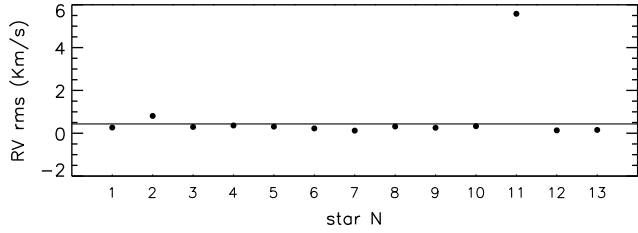


Fig. 7. Radial velocity variations for the Li rich stars (filled circles) compared to the mean variations of the rest of the sample (solid line)

served field, 6 to 8 individual spectra were obtained for different sub-samples, spanning a time window from 30 to 70 days. Star 108191c7 is the only one belonging to a sub-sample observed in only two nights. Figure 7 shows the radial velocity RMS for the Li rich stars, compared to stars with no Li line detected (solid line). Only star 75601c7 shows variations of ~ 6 km/s, about 20 times higher than the others. Due to small sampling and projection effects, we cannot exclude that some other stars are binaries for which we do not detect the variations. However, once again, binarity for *all* the 13 stars would not seem to be the favoured scenario, from the present data.

4.4. Circumstellar material and Infrared excess

In the previous sections we have demonstrated that the Li rich stars we detect are most likely above the RGB bump. In agreement with that, also Kraft et al. (1999) detected an enhanced Li star in M3 (star IV-101 with $A(\text{Li})=4.0$) located 2.25 magnitude brighter than the RGB bump. Monaco & Bonifacio (2008) also found two stars with $A(\text{Li})>3.5-4.0$ close to the RGB tip of the Sagittarius dwarf spheroidal tidal stream.

De la Reza et al. (1996,1997) proposed a different scenario for the Li production along the RGB, associated to short episodes of mass loss occurring just after each extra-mixing event. In this way, some fresh Li would be produced when convection penetrates close to the H-burning shell, which might occur at the RGB bump or brighter. The thin layer containing fresh Li would be quickly carried to the surface (and observed) but it would be lost by the star right afterwards. Observational support to this scenario was given by the detection of infrared excess in some Li-rich giant stars (Gregorio -Hetem et al. 1993, De la Reza et al 1996,1997, Castilho et al. 1998).

Later on, however, Jasiewicz et al. (1999) analyzed 29 giants with infrared excess and did not find any correlation with lithium abundance. In particular, most of their target stars show no detectable Li, 7 of them have abundances compatible with standard dilution ($A(\text{Li})\sim 1.5$), and only one has $A(\text{Li})=3.0$, the latter being indeed close to the RGB bump.

Ideally, mid or far infrared data are needed to detect infrared excess. Since at the moment we do not have such data, we have examined the (J-H,H-K) colour-colour diagram to look for an excess K brightness. As shown by Jones (2008), stars showing a clear excess flux (≥ 1 mag) at $8\mu\text{m}$ with respect to K , also show a ~ 0.4 mag excess brightness in $H-K$ with respect to no-IR-excess stars. Figure 8 shows that no near-IR excess is visible for any of the Li rich stars when compared to the bulk of normal stars in our sample. However, it should be noted that this does not mean that the stars do not have circumstellar material. Indeed,

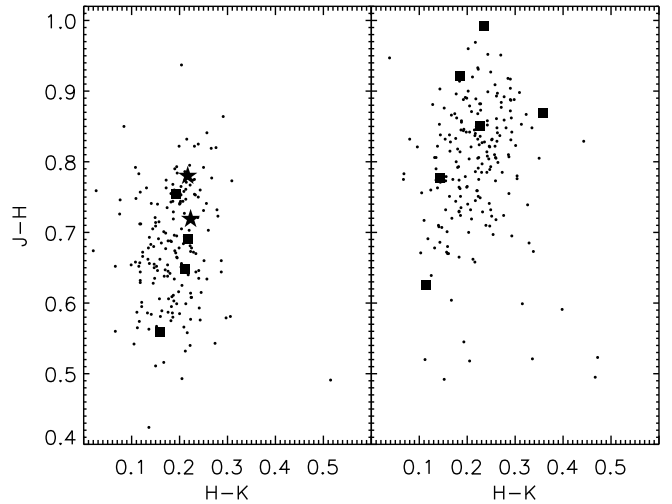


Fig. 8. (J-H,H-K) Colour-colour diagram for the complete sample of stars in the $b = -6^\circ$ field (left) and Baade's Window (right) including the Li rich stars (filled squares). The two most Li-enhanced stars 139560c2 and 111007c8 are plotted as filled stars.

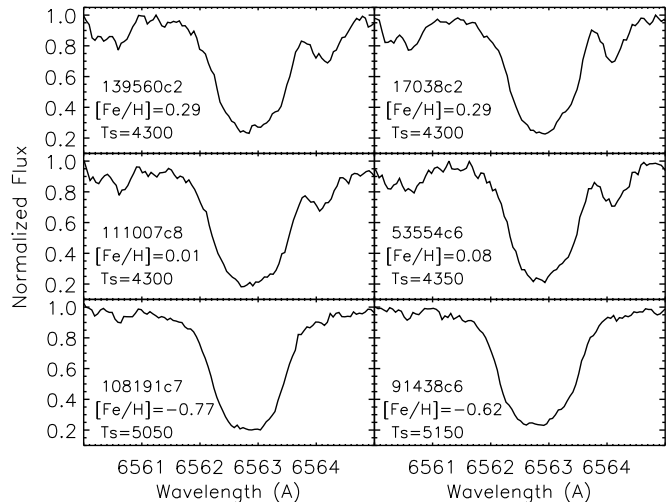


Fig. 9. H_α profile for 3 Li-rich (left panels) and 3 Li-poor (right panel) stars. There are no signs of chromospheric activity in the profiles, nor any other difference between Li-rich and Li-poor stars

as shown Origlia et al. (2007), moderate (~ 0.5 mag) excess in $K - 8\mu\text{m}$ is not detectable in near IR.

Additionally, a significant number of Li rich giants have been found to be also rapid rotators (Drake et al, 2002). However, there is not a one-to-one relation between Li enrichment and rotation (de Medeiros et al. 1996). Furthermore, as found by Drake et al. (2002), this connection only seems to be present when high IR-excess is present. Indication of fast rotation ($v \sin i \geq 8$ km/s) is observed as unusually broad lines in spectral features. In our case, measured FWHM of Li-rich stars show no enhancement when compared to the average of the sample.

Finally, were the high Li abundance related to circumstellar material, we could expect asymmetric wings and/or emission component on the H_α line. Figure 9 shows that this is not observed, as the H_α of Li rich stars (right panels) is identical to that of any other star of the sample (left panels).

5. Conclusions

We have analyzed the Li abundance from a sample of ~ 400 K giants in the galactic bulge. A sub sample of 13 stars present a detectable Li line for which we have measured $A(\text{Li})=0.7\text{-}2.8$.

The sample stars could be divided in three categories:

i) ~ 400 **normal stars** showing no Li line.

ii) **11 Li rich stars** with $A(\text{Li})=0.66\text{-}1.87$. These have abundances compatible with the standard Li dilution occurring at the 1st dredge up. However they seem to have somehow avoided the second extra-mixing episode, further diluting Li after the RGB bump (see Fig.8 in the review by Gratton et al. 2004). These stars show a clear correlation between $A(\text{Li})$ and T_{eff} .

iii) **2 highly Li rich stars** with $A(\text{Li})\sim 2.8$. These stars necessarily underwent a Li production phase.

Most of the proposed explanations for the presence of (a small fraction of) Li rich RGB stars involve the Cameron Fowler mechanism, associated to a deep mixing episode, occurring either at the RGB bump (Charbonnel & Balachandran 2000) or brighter (Sackmann & Boothroyd 1999, Denissenkov & Herwig 2004). From the position of our stars on the CMD we conclude that it is rather unlikely that any of them belongs to the RGB bump, since they are observed to be ~ 1.2 mag brighter than its expected position, at the mean bulge distance.

No clear indication has been found for the presence of a companion to these stars, nor for an infrared excess or some kind of chromospheric activity. By dividing the spectrum of Li rich stars by the one of a *normal* star with similar parameters we could not identify any other spectral feature that might be different between the two.

We have presented more evidence for the presence of Li-rich stars in the first ascent RGB, contrary to the predictions of canonical stellar evolution. None of the proposed explanations could be confirmed here, even though some of them could not be firmly discarded either. Clearly, our poor understanding of this evidences is strongly affected by the small number statistics, partly due to the intrinsic rareness of the phenomenon but also to the lack of a dedicated survey. Specifically designed observations would be needed, ideally in simple stellar populations, in order to establish clearly the evolutionary status of Li-rich giants.

Acknowledgements. We thank Alejandra Recio-Blanco, Angela Bragaglia and Patrick de Laverny for very useful comments and discussions. OG thanks Karin Lind for providing us with the interpolation code and grid for NLTE corrections. MZ and OG acknowledge support by Proyecto Fondecyt Regular #1085278. MZ and DM are partly supported by the BASAL CATA and the FONDAP Center for Astrophysics 15010003.

References

Bensby, T., Feltzing, S., & Lundstrom, I., 2004, A&A, 415, 155
 Boothroyd, A.I. & Sackmann, I.J., 1999, ApJ, 510, 232
 Brown, J.A., Sneden, C., Lambert, D.L. & Dutchover, E. Jr., 1989, ApJS, 71, 293
 Cameron, A.G.W., & Fowler, W.A., 1971, ApJ, 164, 111
 Castilho, B.V., Gregorio-Hetem, J., Spite, F., Barbuy, B. & Spite, M., 2000, A&A, 364, 674
 Charbonnel, C., & Balachandran S.C. 2000, A&AS, 359, 563
 Charbonnel, C., & do Nascimento . 1998, A&AS, 359, 563
 Charbonnel, C., & Zahn, J.P., 2007a, A&A, 467, L15
 Charbonnel, C., & Zahn, J.P., 2007b, A&A, 476, L29
 de La Reza, R., da Silva, L., Drake, N. & Terra, M., 2000, ApJ, 115, 117
 de La Reza, R. & da Silva, L., 1995, ApJ, 439, 917
 de Medeiros, J.R., Melo, C.H.F. & Mayor, M., 1996, A&A, 309, 465
 Denissenkov, P.A. & Herwig, F., 2004, ApJ, 612, 1081
 Denissenkov, P.A., Pinsonneault, M. & MacGregor K.B., 2009, ApJ, 696, 1823
 Domínguez, I., Abia, C., Straniero, O., Cristallo, S., & Pavlenko, Y.V., 2004, A&A 422, 1045

Drake, N.A., de la Reza, R., da Silva, L., Lambert, D.L., 2002, AJ, 123, 2703
 Faraggiana, R., Gerbaldi, M. Molaro, P., & Lambert, D.L., 1991, MmSAI, 62, 189
 Grevesse, N., & Sauval, A.J., 1998, Space Sci. Rev., 85, 161
 Gratton, R.G., & Sneden, C., 1990, A&A, 234, 366
 Gratton, R.G., Sneden, C., Carretta, E., Bragaglia, A., 2000, A&A, 354, 169G
 Gratton, R., & Sneden, C., & Carretta, E. 2004, ARA&A, 42, 385
 Guandalini, R., Palmerini, M., Busso, M. & Uttenthaler, S., 2009,
 Hill, V., & Pasquini, L., 1999, A&A 348, L21
 Iben I.J., 1967, ApJ, 147, 624
 Iben I.J., 1967, ApJ, 147, 650
 Jasiewicz, G., Parthasarathy, M., de Laverny, P. & Thevenin, F., 1999, A&A, 342, 831
 Jones, M.H., 2008, MNRAS, 387, 845
 Kraft, R.P., & Shetrone, M.D., 2000, LIACo 35, 177
 Kurucz, R.L., 1993, CD-ROMs, <http://kurucz.harvard.edu>
 Lecureur, A., Hill, V., Zoccali, et al. 2007, A&A, 465, 799
 Lind, K., Asplund, M., Barklem, P.S., 2009a, A&A accepted, arXiv:0906.0899v1 [astro-ph.SR]
 Lind, K., Primas, F., Charbonnel, C., Grundahl, F., Asplund, M., 2009b, A&A accepted, arXiv:0906.2876v3 [astro-ph.SR]
 Magain, P., 1984, A&A, 134, 189
 McKellar, A. 1940, PASP, 52, 407
 Minniti D., Cook K.H., Vandehei T., Alcock C., Griest K., 1998, ApJ, 499, L175
 Minniti, D. & Zoccali, M., 2008, IAU symposium, 245, 323
 Monaco, L. & Bonifacio, P., 2008, MmSAI, 79, 1
 Origlia, L., Rood, R.T., Fabbri, S., et al., 2007, ApJ, 667L, 850
 Palacios, A., Charbonnel, C., & Forestini, M., 2001, A&A, 375, L9
 Palacios, A., Charbonnel, C., Talon, S., Siess, L., 2006, A&A, 453, 261P
 Pilachowski, C.A., Sneden, C. Harmer, D. & Willmarth, D., 2000, ApJ, 119, 2895
 Pilachowski, C.A., Sneden, C. & Hudek, D., 1990, ApJ, 99, 1225
 Plez, B., 1998, A&A, 337, 495
 Pompeia, L., Barbuy, B., Grenon, M. & Castilho, B.V., 2002, ApJ, 570, 820
 Ramaty, 2001, SSRv 99, 51
 Recio-Blanco, A., de Laverny, P., 2007, A&A, 461, L13
 Reddy, B.E., Lambert, D.L., Laws, C., Gonzalez, G. & Covey, K., 2002, MNRAS, 335, 1005
 Sackmann, I., & Boothroyd, A.I. 1999, ApJ, 510, 217
 Smith, V.V., Plez, B., Lambert, D.L., & Lubowich, D.A., 1995, ApJ, 441, 735
 Spite, F. & Spite, M., 1982, A&A, 115, 357
 Stetson, P.B. & Pancino E., 2008, PASP, 120, 1332
 Uttenthaler, S., Lebzelter, T., Palmerini, et al., 2007, A&A, 471, L41
 Zoccali, M., Cassisi, S., Piotto, G., Bono, G. & Salaris, M. 1999, ApJ, 518, L49
 Zoccali, M., Lecureur, A., Barbuy, B., et al., 2006, A&A, 457, L1
 Zoccali, M., Lecureur, A., Hill, V. et al., 2008, A&A, 486, 177